*Polish Journal of Chemical Technology, 16, **4**, 55 — 59, 10.2478/pjct-2014-0070*

Ozone decomposition on ZnO catalysts obtained from different precursors

Katya I. Milenova[1*], Penko M. Nikolov[2], Nikoleta A. Kasabova[2], Ivalina A. Avramova[3]

[1] *Bulgarian Academy of Sciences, Institute of Catalysis, Acad. G. Bonchev Str., bl 11, Sofia 1113, Bulgaria*
[2] *University of Chemical Technology and Metallurgy, 8 Kliment Ohridski, 1756, Sofia, Bulgaria*
[3] *Bulgarian Academy of Sciences, Institute of General and Inorganic Chemistry, Akad. G. Bontchev str. bl 11, 1113, Sofia, Bulgaria*
[*]*Corresponding author: e-mail: kmilenova@mail.bg*

Kinetic investigations for ozone conversion on three different series of zinc oxide catalysts, containing pure ZnO and doped with Mn or Cu one with dopant content less than 1 wt.% were carried out. The different samples were obtained from carbonate, nitrate and acetate precursors. The as prepared catalysts were characterized by AAS, XRD, IR, EPR and BET methods. The mean size of the crystallites determined by XRD data is in the range 27÷68 nm. The presence of Mn^{2+} and Cu^{2+} ions into the ZnO matrix was established by EPR. The ozone decomposition was investigated for 30÷75°C temperature range. The zinc carbonate precursor samples show highest activity, while the nitrate precursor ones show lowest activity toward reaction decomposition of ozone in the whole temperature range. At 75°C two of the catalyst, obtained from carbonate precursor – ZnO and CuZnO show 100% conversion.

Keywords: ozone decomposition, zinc oxide catalyst, manganese doping, copper doping, nanosize.

INTRODUCTION

Zinc oxide is a catalyst, preferred for many heterogenic reactions due to its insolubility and low price[1]. One of its major applications is for decomposition of ozone, initially used for oxidation of different organic compounds in liquid phase[2, 3, 4, 5, 6, 7]. The catalytic activity of ZnO strongly depends on the used method of synthesis[5, 6, 7, 8]. The specific surface area and the defects have great influence on the activity of metal oxides catalysts. For achieving higher activity different transition metal dopants such as Mn or Cu could be used for raising surface defects leading to evolution of the specific surface area of the catalysts. It is well known that Mn and Cu substitute Zn ions in the structure of hexagonal wurzite ZnO[9, 10]. Well evolved surface area typical for nanomaterials has advance on catalysis. Decrease of the mean size of the particles and respectively increase of the specific surface area leads to increase in the number of active sites, where the reaction is carried out[11]. The scarce information describing the way of synthesis of ZnO catalysts used for ozonation exists in the literature[5]. Few publications discussed the application of pure ZnO as catalyst for ozone decomposition as well as for disposal of organic pollutants in the presence of ozone. However the use of doped with small amounts of Mn and Cu zinc oxide as ozone decomposition catalyst is not investigated from other authors. In previous publication[12] we have made investigation of the activity of doped ZnO for ozone decomposition with the time. The aim of the present article is to explore the influence of the precursor used for obtaining of ZnO doped with Mn and Cu over catalytic activity for ozone decomposition with the temperature.

EXPERIMENTAL

Pure and doped with Mn and Cu zinc oxide samples were obtained from zinc nitrate, acetate and carbonate precursors. For preparation of ZnO from nitrate and acetate 15 g of $Zn(NO_3)_2 \cdot 4H_2O$ and 15 g of $Zn(CH_3COO)_2 \cdot 2H_2O$ were dissolved in 100 ml H_2O, respectively. The as prepared solutions were decomposed under electromechanical stirring at 1000 rpm and temperature 150°C. For the doped samples 0.25 M $Mn(NO_3)_2$ or 0.25 M $Cu(NO_3)_2$ stock solutions were also added into $Zn(NO_3)_2 \cdot 4H_2O$ or $Zn(CH_3COO)_2 \cdot 2H_2O$ solutions. The concentration of each metal dopant was so calculated as to give 0.15 wt% content with respect to Zn. As final preparation step all samples were dried first at room temperature, then at 100°C for an hour and finally calcinated at 500°C for 3 h in air at atmospheric pressure.

In the case of carbonate precursor undoped and doped with Cu or Mn zinc oxide samples were prepared by precipitation method. Analytical grade of purity zinc sulfate (heptahydrate) $ZnSO_4 \cdot 7H_2O$, sodium carbonate Na_2CO_3 and 0.25 M $CuSO_4$ stock solution or manganese sulfate 0.25 M $MnSO_4$ stock solution were used as starting materials. In a typical experiment we dissolved 90 g of Na_2CO_3 in 850 ml H_2O under heating and continuous stirring (solution 1). An amount of 20 g $ZnSO_4 \cdot 7H_2O$ was dissolved in 140 ml H_2O under heating and continuous stirring (solution 2). Calculated quantities of copper sulfate were added to the solution 2 such to obtain mixture of ZnO doped with 0.15 wt.% Cu or Mn. This mixed solution of $ZnSO_4 \cdot 7H_2O$ and $CuSO_4 \cdot H_2O$ or $MnSO_4 \cdot H_2O$ was added drop by drop to the solution 1. After adjusting the pH value to 11, the final mixture solution was stirred under heating for 10 minutes. The precipitate was separated by filtration, washed several times with distilled water to pH value 7 and dried in air. For preparation of final crystal samples they were dried at room temperature, then at 100°C for an hour and finally calcinated at 500°C for 3 h in air at atmospheric pressure.

Several samples were prepared and named as follows:

From nitrate precursor: ZnO(nit.), MnZnO(nit.) and CuZnO(nit.),

From acetate precursor: ZnO(ac.), MnZnO(ac.) and CuZnO(ac.),

From carbonate precursor: ZnO(ca.), MnZnO(ca.) and CuZnO(ca.).

The synthesis is published in details in[12].

Sample characterization

AAS analysis

Chemical composition of the samples was determined using Atomic Absorption Analysis FAAS - SOLAAR M5 spectrometer. For preparation of standard solutions standards produced by "Titrisol" (Merck) – Germany were used, the concentration of reference metal content was 1000 ppm.

X-ray diffraction (XRD) analysis

The X-ray diffraction (XRD) analysis was carried out on a Siemens powder diffractometer model D500 using CuKα radiation within a 2θ angle of diffraction interval of 10–60 degrees. The identification of the phases was done by means of the JCPDS database of the International Center of Powder Diffraction Data. The particle size was determined by Scherrer's formula.

Infrared Spectroscopy (IR)

The IR spectra were recorded in the range of 4000 to 400 cm^{-1} on a IFS 25 spectrometer (Brűker) with resolution of less than 2 cm^{-1}. The samples were prepared as tablets from KBr, with content of investigated samples.

Electron paramagnetic resonance (EPR)

The electron paramagnetic resonance (EPR) spectra were registered as a first derivative of the absorption signal in the temperature interval of 100–400 K using an ERS 220/Q instrument.

Adsorption – texture analysis

The determination of the specific surface area was carried out by nitrogen adsorption at the boiling temperature of liquid nitrogen (77.4 K) using a conventional volume-measuring apparatus. Before the measurements, the samples were degassed at 423K until the residual pressure became lower than 1.333 x 10^{-2} Pa.

Catalytic activity test

The catalytic activity of the sample in the reaction of ozone decomposition was investigated in a plug flow reactor system. The catalyst particle sizes were 0.25÷0.6 mm. The volume rate was 120 000 h^{-1}. Ozone was synthesized in a flow of oxygen (99.7%) and dried with silica gel using an ozone generator with silent discharge and coaxial electrodes. The inlet concentration of ozone was varying from 13 to 15 g/m^3 (0.25–0.3 mol/m^3). Ozone concentration was measured by an Ozomat GM (Anseros, Germany) ozone analyzer with a resolution of ± 0.1 g/m^3. The range of the temperature was 30÷75°C, the raise step was 5 degrees per 2 minutes.

RESULTS AND DISCUSSION

The X-ray diffraction patterns of investigated pure and doped by Cu and Mn zinc oxide synthesized from carbonate, nitrate and acetate precursors are shown in Figures 1÷3. The X-ray diffraction analysis revealed the formation of hexagonal wurzite ZnO phase (JCPDS 36-1451).

There is no indication of any secondary phase or clusters, confirming that the samples are only one single phase. The XRD results also indicate that the Mn^{2+} and Cu^{2+} ions systematically substituted the Zn^{2+} ions in the samples without changing the wurtzite structure. This is due to the fact that ionic radius of Cu^{2+} (0.73 Å) is very close to that of Zn^{2+} (0.74 Å), due to which Cu can easily penetrate into ZnO crystal lattice, as well as the fact that the ionic radius of Mn^{2+} is 0.80 Å, whereas that of Zn^{2+} is 0.74 Å. The slight shift to low angular scale is clearly evident for the most intense diffraction peak in a case of doping by Cu or Mn ions. Additionally, the intensity of the diffraction peaks decreases, and the width broadens due to the formation of smaller grain diameters as a result of an increase in disorder in ZnO due to Cu^{2+} or Mn^{2+} doping. The shifting and broadening of XRD lines with doping strongly suggest that Cu^{2+} and Mn^{2+}, respectively successfully substituted Zn^{2+} into the ZnO host structure. The sizes of crystallites are calculated for all investigated samples by Debye-Sherrer equation and the results are presented in the Table 1.

Table 1. Type of the used precursor, dopant content, crystallites size and specific surface area (A_{BET}) of undoped ZnO and Mn-doped and Cu-doped ZnO

Sample	Dopant content, [wt.%]	Crystallites size, [nm]	A_{BET}, [m^2/g]
ZnO(ac.)	–	42	8
MnZnO(ac.)	0.16	39	9
CuZnO(ac.)	0.19	35	10
ZnO(ca.)	–	31	22
MnZnO(ca.)	0.13	28	23
CuZnO(ca.)	0.18	27	26
ZnO(nit.)	–	68	1
MnZnO(nit.)	0.14	65	3
CuZnO(nit.)	0.17	57	5

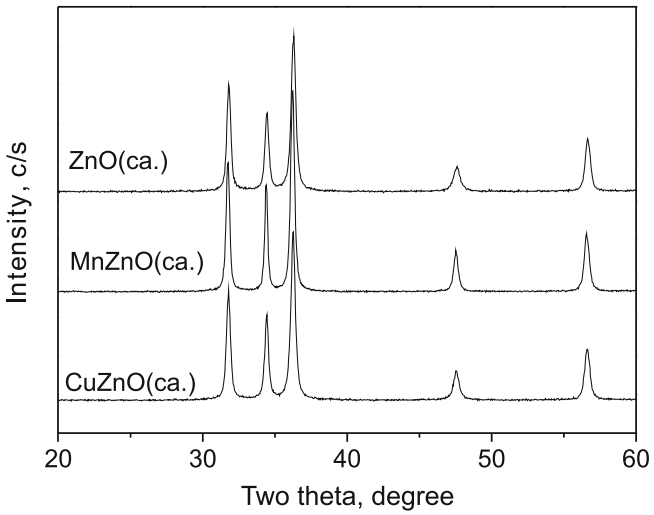

Figure 1. X-ray diffraction patterns of samples obtained from carbonate

The compositions of the obtained samples and their specific surface area are presented in Table 1. The concentration of the dopants was evaluated by AAS method and is less than 0.2 wt.%. It can be seen that specific surface area strongly depends on precursor type. The lowest specific surface area has ZnO obtained from zinc nitrate precursor. The reasonable explanation for this could be associated with the fact that the process of decomposition of the precursor pass through in a molten state. Highest specific surface area has ZnO obtained from carbonate precursor, due to the fact that during decomposition process a great amount of gases is dissociated. That difference in the value of the specific surface area keeps for doped with Mn and Cu zinc oxide samples. ZnO(ca.) samples have highest specific

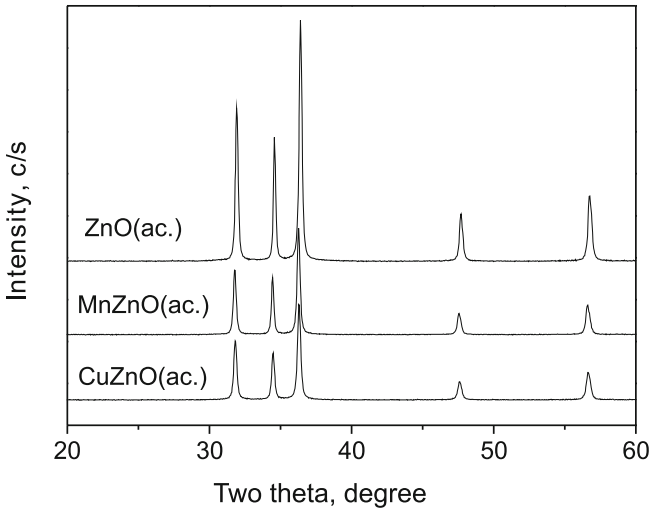

Figure 2. X-ray diffraction patterns of samples obtained from acetate

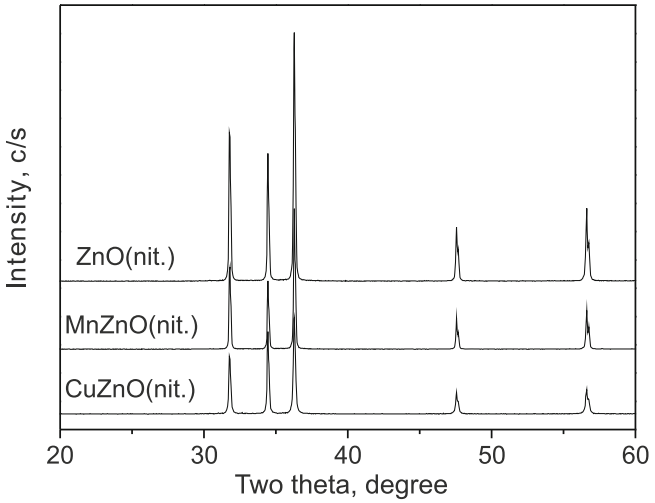

Figure 3. X-ray diffraction patterns of samples obtained from nitrate

area – 22÷26 m^2/g, ZnO(ac.) ones have 8÷10 m^2/g and the ZnO(nit.) samples have the lowest area – 1÷5 m^2/g. All obtained samples are nanosized ones. Calculated size of the crystallites from X-Ray data is in the range of 27÷68 nm. Doping with Mn and Cu leads to slight decrease of the crystallite sizes compared to pure ZnO.

IR spectroscopy results (see Figs. 4 and 5) of Mn and Cu doped samples, obtained from nitrate, carbonate and acetate precursors show absorption peak in the range 520÷420 cm^{-1}, which is typical characteristic absorption band of ZnO[13]. O-Cu-O bonding causes bending close to 500 cm^{-1} and 1384 cm^{-1} (Fig. 5)[14, 15].

The EPR spectra of MnZnO samples are shown in Figure 6. Six characteristic lines for isolated Mn^{2+} are observed for MnZnO(ca.) and MnZnO(ac.) samples, together with broad line of cluster manganese ions, as mentioned in[16, 17, 18]. According to the spectroscopic analysis the manganese ions are dispersed within the ZnO matrix, and adsorbed on the ZnO surface, or formed manganese clusters with strong metal-metal interactions[5]. The six-line hyperfine structure is clear indication for interaction between nucleus and the electrons in the magnetic field[19]. EPR spectrum of ZnO(nit.) shows only broad line of cluster Mn ions as it was established by Bogomolova et al.[20]. The EPR spectra of CuZnO catalysts are presented in the next Figure 7. For all of

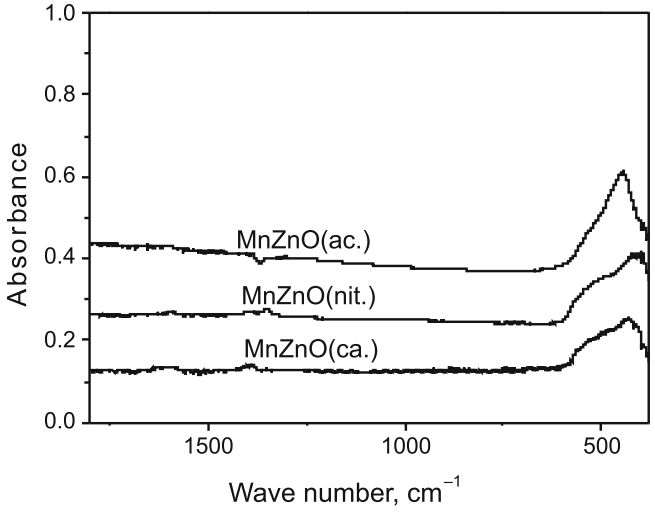

Figure 4. IR spectroscopy of MnZnO(ac.); MnZnO(nit.); MnZnO(ca.)

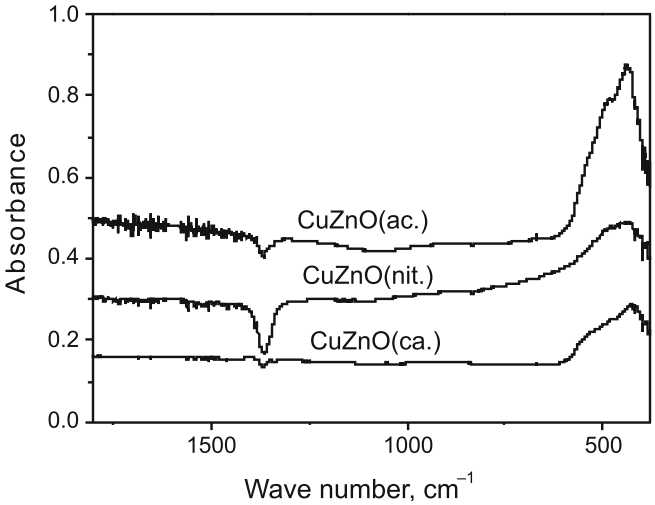

Figure 5. IR spectroscopy of CuZnO(ac.); CuZnO(nit.); CuZnO(ca.)

the investigated samples mainly isolated Cu^{2+} ions have been registered[21]. Similar results for Cu^{2+} ions distribution were discussed in[20]. Furthermore for CuZnO(ac.) sample narrow signal with g-factor about 2.0 was observed. This signal most probably is due to the formation of different radicals during the process of decomposition of acetate ligand.

The ozone decomposition versus temperature for the pure ZnO samples as well as for Cu doped samples is

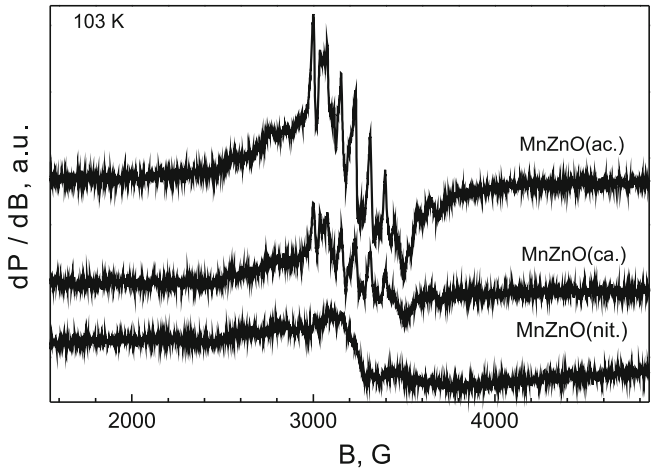

Figure 6. EPR spectra of: MnZnO(nit.); MnZnO(ca.); MnZnO(ac.)

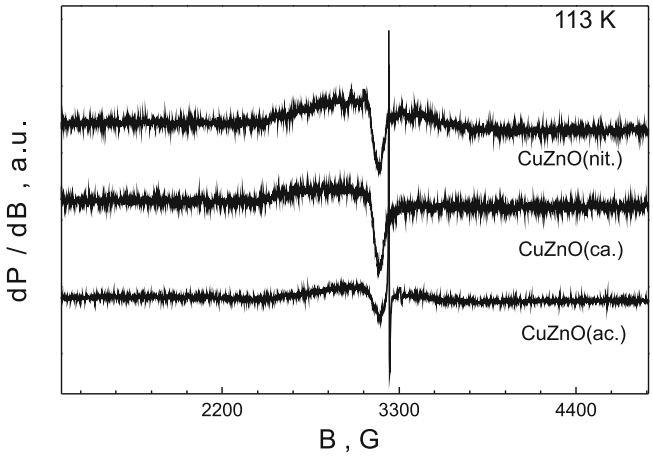

Figure 7. EPR spectra of: (a) CuZnO(nit.); (b) CuZnO(ca.); (c) CuZnO(ac.)

presented in Figure 8. Two main conclusions can be made from the obtained results. First of all the obtained carbonate precursor samples have considerably higher conversion compared to those of nitrate and acetate precursor samples, which easily can be explained with their well developed specific surface area, as a result of dissociation of great amount of gases during their synthesis. The conversion for carbonate precursor samples is not proportionally higher to the specific surface area compared to other precursor samples most probably due to internal diffusion factors. Practically full conversion is observed only for carbonate precursor synthesized samples in a temperature interval 70÷75°C, while the most active acetate sample has less than 66% conversion in this temperature range. Reasons for the activity of ZnO as catalyst are – its donor characteristic, caused by the large number of defect sites as oxygen vacancies and interstitial atoms and the acceptor states arising from vacancies and interstitial oxygen atoms[22].

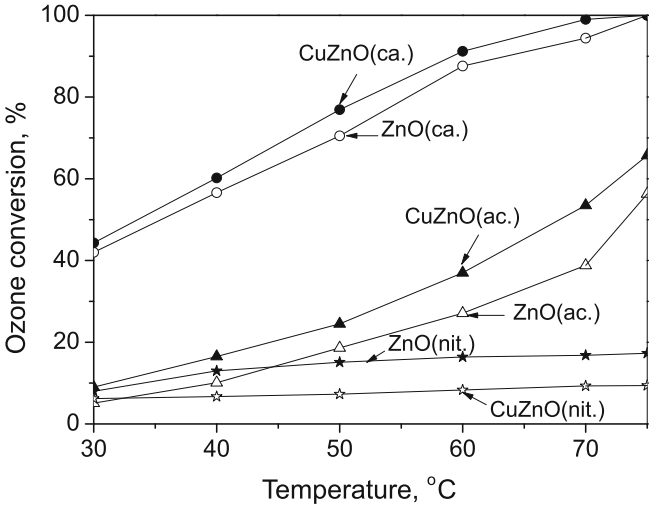

Figure 8. Ozone conversion with the temperature for pure ZnO and Cu doped ZnO samples obtained from acetate, nitrate and carbonate precursors

Another important conclusion is that doping of zinc oxide with very little quantities of copper considerably raises catalytic activity for ozone decomposition. The light-off conversion for CuZnO(ca.) is reached at about 34°C, compared to 36°C for pure ZnO(ca.). The comparison for acetate precursor samples show that the light--off temperature for the copper doped one is reached at 68°C against 74°C for undoped one. Noticeable raise of the activity is observed for nitrate precursor synthesized samples too, but because their specific surface areas are not well developed, the obtained catalysts according to us cannot find practical application. Bellini et al.[10] find out that diffusion processes during the method of obtaining of the catalysts at high temperatures could lead to reactions that may provoke the appearance of defects when Cu^{2+} cations substitute Zn^{2+} cations in the crystal lattice of ZnO. It was also observed (see the explanation above) that by doping with Cu the intensity of the diffraction peaks of the ZnO decreased which was caused by the decrease in the crystallinity of ZnO. Such changes in crystallinity might be the result of changes in the atomic environment due to extrinsic doping of ZnO samples. According to theoretical calculations by Yan et al.[23] on Cu-ZnO electronic structure, Cu occupying a Zn site creates a single-acceptor state above the valence band Ev of ZnO. According to our experimental XRD results, only ZnO peaks have been detected, which suggest that Cu is incorporated into the lattice. The Cu doping mechanism of ZnO can be described by Cu-doping into the ZnO host lattice; Cu^{2+} is substituting the Zn^{2+} sites. In our previous paper[24] the X-ray Photoelectron Spectroscopy (XPS) analysis was employed on the same system but synthesized from different precursor. We have observed a significant increase in the ratio of the oxygen XPS features attributed to defective ZnO in the Cu-doped sample as compared to the undoped ZnO reemphasizing the incorporation of Cu^{2+} ions into the ZnO and the consequent generation of defects. The result shows that the high activity of Cu doped zinc oxide is due to the creation of complex defects in the ZnO lattice[10].

Practically similar conversion of the manganese doped and pure ZnO (not shown here) catalyst was reached and this fact limits their application for ozone decomposition.

CONCLUSIONS

The catalytic activity of the catalysts, obtained from pure or doped with Cu and Mn zinc oxide is determined by means of the initial precursor used as follows: carbonate>acetate>nitrate.

The same correlation is observed and is related to the physicochemical parameters of the investigated catalytic systems – specific surface area and size of crystallites.

The catalyst based on CuZnO (ca.) is the most perspective for practical application, reaching 100% ozone conversion at 70°C.

LITERATURE CITED

1. Naik, S.P. & Fernandes, J.B. (1999). Temperature programmed desorption studies on a new active zinc oxide catalyst. *Thermochim. Acta* 332(1), 21–25. DOI: 10.1016/S0040-6031(99)00063-5.

2. Huang, W.J., Fang, G.C. & Wang, C.C. (2005). A nanometer-ZnO catalyst to enhance the ozonation of 2,4,6-trichlorophenol in water. *Coll. Surf. A*, 260, 45–51. DOI: 10.1016/j.colsurfa.2005.01.031.

3. Jung, H., Choi, H. (2006). Catalytic decomposition of ozone and para – Chlorobenzoic acid (pCBA) in the presence of nanosized ZnO. *Appl. Catal. B*, 66, 288–294. DOI: 10.1016/j.apcatb.2006.03.009.

4. Zhai, X., Chen, Z., Zhao, S., Wang, H. & Yang, L. (2010). Enhanced ozonation of dichloroacetic acid in aqueous solution using nanometer ZnO powders. *J Environ. Sci.*, 22(10) 1527–1533. DOI: 10.1016/S1001-0742(09)60284-9.

5. Muruganandham, M. & Wu, J. (2008). Synthesis, characterization and catalytic activity of easily recyclable zinc oxide nanobundles. *Appl. Catal. B. Environ.,* 80, 32–41. DOI: 10.1016/j.apcatb.2007.11.006.

6. Dong, Y., Wang, G., Jiang, P., Zhang, A., Yue, L., Zhang, X. (2011). Simple preparation and catalytic properties of ZnO for ozonation degradation of phenol in water, *Chin. Chem. Lett.*, 22, 209–212. DOI: 10.1016/j.cclet.2010.10.010.

7. Xu, Z., Ben, Y., Chen, Z. & Qi, F. (2013). Facile synthesis of snowflake-like ZnO nanostructures at low temperature and their super catalytic activity for the ozone decomposition. *Mater. Res. Bull.*, 48, 1725–1727. DOI: 10.1016/j.materresbull.2012.11.095.

8. Chauvin, S., Saussey, J., Lavalley, J. & Djega-Mariadassou, G. (1986). Definition of polycrystalline ZnO catalytic sites and their role in CO hydrogenation. *Appl. Catal.* 25(1–2), 59–68. DOI: 10.1016/S0166-9834(00)81222-1.

9. Rekha, K., Nirmala, M., Nair, M. & Anukaliani, A. (2010). Structural, optical, photocatalytic and antibacterial activity of zinc oxide and manganese doped zinc oxide nanoparticles. *Physica B*, 405, 3180–3185. DOI: 10.1016/j.physb.2010.04.042.

10. Bellini, J., Morelli, M. & Kiminami, R. (2002). Electrical properties of polycrystalline ZnO: Cu obtained from freeze--dried ZnO + copper (II) acetate powders *Mater. Sci. Mater. Electron.* 13 (8), 485–489, DOI: 10.1023/a:1016160204435.

11. Dodd, A., McKinley, A., Tsuzuki, T. & Saunders, M. (2009). Tailoring the Photocatalytic Activity of Nanoparticulate Zinc Oxide by Transition Metal Oxide Doping. *Mater. Chem. Phys.* 114, 382–386. DOI: 10.1016/j.matchmphys.2008.09.041.

12. Nikolov, P., Milenova, K. & Mehandjiev, D. (2008). Decomposition of ozone over pure and doped with Cu and Mn zinc oxide. *C. R. Acad. Bulg. Sci.* 61, 1127.

13. Xie, J., Li, Y., Zhao, W., Bian, L. & Wei, Y. (2011). Simple fabrication and photocatalytic activity of ZnO particles with different morphologies. *Powder. Tech.,* 207, 140–144. DOI: 10.1016/j.powtec.2010.10.019.

14. Saedy, S., Haghighi, M. & Amirkhosrow, M. (2012). Hydrothermal synthesis and physicochemical characterization of $CuO/ZnO/Al_2O_3$ nanopowder. Part I: Effect of crystallization time. *Particuology* 10, 729–736. DOI: 10.1016/j.partic.2012.05.001.

15. Hung, C. (2009). Synthesis, characterization and performance of CuO/La_2O_3 composite catalyst for ammonia catalytic oxidation. *Powder. Tech.,* 196, 56–61. DOI: 10.1016/j.powtec.2009.07.001.

16. Diaconu, M., Schmidt, H., Pöppl, A.R., Böttcher, R., Hoentsch, J., Rahm, A., Hochmuth, H., Lorenz, M. & Grundmann, M. (2005). EPR study on magnetic $Zn_{1-x}Mn_xO$. *Superlat. Microst*. 38, 413–420. DOI: 10.1016/j.spmi.2005.08.012.

17. Singh, S., Chakradhar, R., Rao, J. & Karmakar, B., (2010). EPR, optical absorption and photoluminescence properties of MnO_2 doped $23B_2O_3$–5ZnO–$72Bi_2O_3$ glasses. *Physica B*, 405, 2157–2161. DOI: 10.1016/j.physb.2010.01.123.

18. Clavel, G., Willinger, M., Zitoun, D. & Pinna, N., (2007). Solvent Dependent Shape and Magnetic Properties of Doped ZnO Nanostructures. *Adv. Funct. Mater.*, 17(6), 3159–3169. DOI: 10.1002/adfm.200601142.

19. Vethanathan, S., Brightson, M., Sundar, S. & Perumal, S., Synthesis of Mn doped ZnO nanocrystals by solvothermal route and its characterization. (2011). *Mater. Chem. Phys.*, 125, 872–875. DOI: 10.1016/j.matchemphys.2010.09.029.

20. Bogomolova, D., Jachkin, A., Krasil'nikova, A., Bogdanov, L., Fedorushkova, B. & Khalilev, D. (1990). EPR of transition metals in fluoroaluminate glasses. *J. Non-Crystall Solids*. 125, 32–39. DOI: 10.1016/0022-3093(90)90320-L.

21. Srinivasan, G. & Kumar, J. (2008). Effect of Mn-doping on the microstructures and optical properties of sol gel derived ZnO thin films. *J. Cryst. Growth*. 310, 1841–1846. DOI: 10.1016/j.jcrysgro.2007.10.056.

22. Xu, C., Cao, L., Su, G., Liu, W., Liu, H., Yu, Y. & Qu, X. (2010). Preparation of ZnO/Cu_2O compound photocatalyst and application in treating organic dyes. *J. Hazard. Mater*. 176, 807–813. DOI: 10.1016/j.jhazmat.2009.11.106.

23. Yan, Y., Al-Jassim, M.M. & Wei, S.H. (2006). Doping of ZnO by group-IB elements, *Appl. Phys. Lett.* 89, 181912. DOI: /10.1063/1.2378404.

24. Milenova, K., Avramova, I. & Nikolov, P. (2013). Nanosized Cu/ ZnO catalytic systems –Characterization and activity toward ozone decomposition, *J. Inter. Sci. Public.: Mater., Met. Technol.*, 7, Part 2, 462–471.